Proceedings of the 20th International Conference on Soil Mechanics and Geotechnical Engineering– Rahman and Jaksa (Eds)

Flow liquefaction triggering analyses of a tailings storage facility by means of a simplified numerical procedure

Liquéfaction en flux déclenchant des analyses d'une installation de stockage de résidus au moyen d'une procédure numérique simplifiée

Mauro G. Sottile, Ignacio A. Cueto & Alejo O. Sfriso
SRK Consulting Argentina and Universidad de Buenos Aires. Chile 300, Buenos Aires, Argentina.

Osvaldo N. Ledesma & Arcesio Lizcano
SRK Consulting North America. 1066 West Hastings Street, Vancouver, Canada

ABSTRACT: Recent failures of upstream-raised tailings storage facilities (TSF) resulted in higher standards required by the mining industry on assessing the risk of tailings flow liquefaction. Standard industry practice entails the use of limit equilibrium analyses to compute a factor of safety -or, in the best case, a probability of failure- assuming peak or residual undrained shear strength ratios; this procedure, however, fails to account for the effect of strain-softening and brittleness, as it neglects the work input required to drive the softening process that leads to a progressive failure. This paper applies a numerical procedure to evaluate the flow liquefaction triggering of a real TSF; the methodology entails the use of finite element models employing the Hardening Soil model with small-strain stiffness, calibrated for this purpose by focusing on the stiffness parameters that control the evolution of shear-induced plastic volumetric strains; this calibration is able to effectively reproduce the stress-strain curve in undrained shearing, including the peak and residual undrained shear strength ratios and their associated deformations. In the example shown, a TSF construction sequence is modelled in detail and subsequent trigger analyses are carried out for several scenarios, including: an undrained load at the dam crest, to represent a rapid embankment raise; and a contraction at the toe, to represent eventual movements due to creep or operational accidents. Results show that this numerical modelling is useful to evaluate the flow liquefaction potential of the facility and to validate its robustness after the construction of a reinforcement buttress.

RÉSUMÉ : Les défaillances récentes des installations de stockage des résidus surélevées en amont (TSF) ont entraîné des normes plus élevées exigées par l'industrie minière pour évaluer le risque de liquéfaction du flux de résidus. La pratique courante de l'industrie implique l'utilisation d'analyses d'équilibre limite pour calculer un facteur de sécurité - ou, dans le meilleur des cas, une probabilité de défaillance - en supposant des rapports de résistance au cisaillement maximal ou résiduel non drainé; cette procédure, cependant, ne tient pas compte de l'effet de l'adoucissement de la déformation et de la fragilité, car elle néglige le travail nécessaire pour conduire le processus de ramollissement qui conduit à une défaillance progressive. Cet article applique une procédure numérique pour évaluer le déclenchement de liquéfaction en flux d'une TSF réelle; la méthodologie implique l'utilisation de modèles par éléments finis utilisant le modèle de sol durcissant à faible rigidité de déformation, calibré à cet effet en se concentrant sur les paramètres de rigidité qui contrôlent l'évolution des déformations volumétriques plastiques induites par cisaillement; cet étalonnage est capable de reproduire efficacement la courbe contrainte-déformation en cisaillement non drainé, y compris les rapports de résistance au cisaillement maximal et résiduel non drainé et leurs déformations associées. Dans l'exemple illustré, une séquence de construction TSF est modélisée en détail et des analyses de déclenchement ultérieures sont effectuées pour plusieurs scénarios, dont: une charge non drainée à la crête du barrage, pour représenter une montée rapide du remblai; et une contraction au niveau des orteils, pour représenter les mouvements éventuels dus au fluage ou aux accidents de fonctionnement. Les résultats montrent que cette modélisation numérique est utile pour évaluer le potentiel de liquéfaction en flux de l'installation et pour valider sa robustesse après la construction d'un contrefort de renforcement.

KEYWORDS: Flow liquefaction, triggering analyses, tailing storage facilities, Plaxis 2D, HSS.

1 INTRODUCTION

Tailings are man-made materials created from mine-rock crushing, generally deposited hydraulically as a slurry into storage facilities (TSFs). The lack of compaction after deposition and the electrical interaction among finer particles leads to loose material arrangements, which can be locked by diagenesis at early stages.

Despite being attractive from an economical perspective, recent upstream-raised TSFs failures -such as Samarco and Brumadinho (Santamarina, 2019)- have depicted their vulnerability against flow liquefaction. This phenomenon occurs when loose water-saturated tailings undergo a sudden loss of strength due to undrained shearing or by internal fabric collapse, produced by external actions collectively called “trigger events”. Due to difficulties in identifying and estimating the probability of occurrence of these triggering events, international guidelines (e.g. ANCOLD, 2019) recommend to conservatively assume that flow liquefaction will occur for brittle/contractive saturated tailings. Thus, one scenario of current design practice involves limit equilibrium (LE) analyses adopting fully softened shear strength. While safe, this approach fails to account for the effect of strain-softening and brittleness, as it neglects the work input required to drive the softening process that leads to a progressive failure (i.e., too conservative).

This paper applies the procedure proposed by Sottile et. al. (2020) to the evaluation of liquefaction triggering of a real TSF and to the design of a reinforcement buttress. The methodology entails: i) the estimation of the state parameter distribution within the tailings body using CPTu data; ii) the calibration of the Hardening Soil model with small-strain stiffness (HSS) to account for strain-softening undrained shear; iii) the analysis of the overall performance of the dam after imposing two triggering mechanisms: a load at the dam crest and a deformation at the toe of the upstream raise. Finally, the dam response is evaluated for a reinforced configuration after building a buttress.

2 CASE STUDY

The case study is a 72m-high tailings retention structure that was built using a combination of downstream and upstream methods (Figure 1). The construction sequence can be summarized as follows: i) a 45m-high starter dam with a central clay core is built; ii) tailings are deposited as a slurry behind the starter dam; iii) rockfill and embankment raises are placed on top of the starter dam to increase the dam capacity; iv) tailings are deposited as a slurry until reaching the downstream dam crest; v) successive upstream raises are completed with subsequent tailings deposition until the dam reaches its current height.

CPTu tests were executed along the current dam crest. The interpreted data suggests that tailings are predominantly contractive and near saturated materials; thus, susceptible to flow liquefaction. Limit equilibrium analyses show that the factors of safety for the current situation does not comply with international guidelines and a reinforcement buttress is needed to achieve adequate margins of safety.

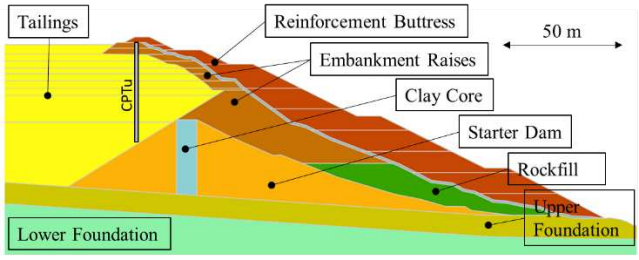

Figure 1. TSF representative cross-section and zoning.

3 TAILINGS CHARACTERIZATION

3.1 *Field and laboratory testing*

A field and laboratory geotechnical testing program was carried out to characterize the mechanical behavior of the tailings. General laboratory characterization tests results are summarized as follows: i) the sand content ranges from 52% to 82% and the fines content ranges from 18% to 47%; ii) there is a reduced gravel fraction (less than 5%), which comes from the earth fill material; iii) the liquid limit of the fine fraction ranges from 19% to 31%, and plasticity index from 0% to 14%; iv) specific gravity ranges from 2.67 to 2.94.

Isotropically consolidated undrained triaxial compression tests (CIUC) were performed, which are used to determine the drained strength parameters. Four CPTu soundings were executed along the current dam crest; the results are used to determine the state parameter ψ and the residual shear strength ratio $s_{u,res}/\sigma'_v$ distributions on the upper 40 m of the tailings as shown in the following sections.

3.2 *State parameter*

The state parameter ψ was computed along the four CPTu soundings using two screening methods: Robertson (2010) and Jefferies & Been (2016) with Plewes (1992) correlation. Results are shown in Figure 2. The limit $\psi = -0.06$ is used to distinguish contractive from dilative behavior. All soundings entail predominantly contractive behavior with values around $\psi \cong 0.0$ and isolated peaks up to $\psi = 0.25$. A good agreement between the two screening methods is observed, with slightly higher values obtained with Robertson (2010).

Depth ranges, limited by the pre-drilling and the inferred position of the starter dam, were selected to perform frequency analyses. Based on these statistical analyses (Figure 3) it is observed that more than 90% of the tailings are contractive (i.e. $\psi > -0.06$), 50-70% of the tailings have $\psi > 0.0$. A design value $\psi = 0.02$, with a likelihood of occurrence of 65-70% was selected .

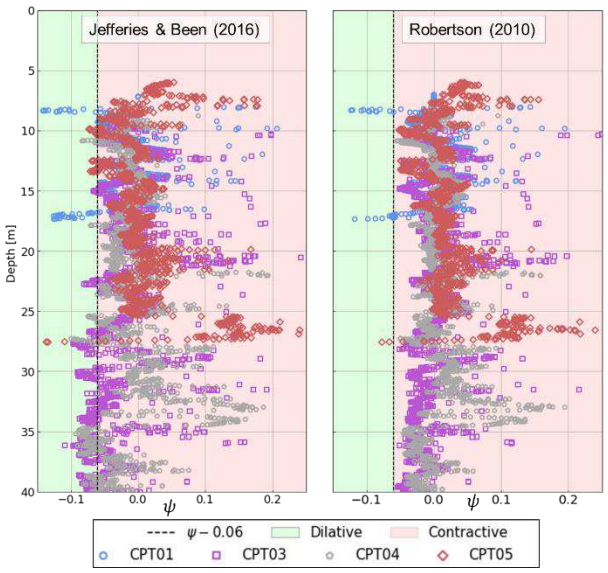

Figure 2. State parameter distribution at each CPTu sounding. After Jefferies & Been (2016) and Robertson (2010).

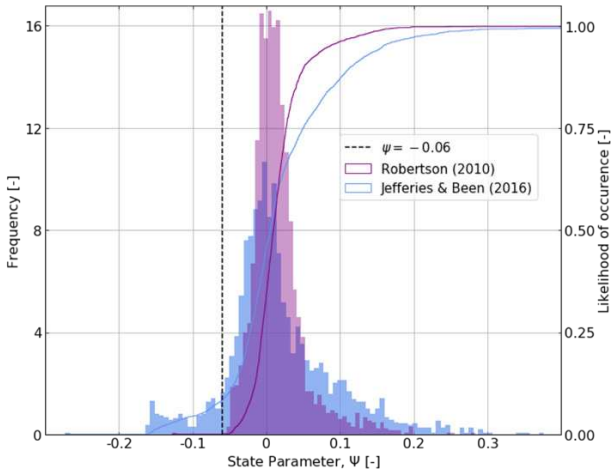

Figure 3. State parameter frequency and cumulative frequency analysis.

3.3 *Residual shear strength ratio*

The residual shear strength $s_{u,res}$ is estimated to be the sleeve friction f_s of the CPTu. This is a conservative lower bound, due to the reduced friction of the soil-to-steel surface for a polished cone (Robertson, 2009). $s_{u,res}$ increases almost linearly with depth so the normalization by the vertical effective stress produces an almost constant residual shear strength ratio $s_{u,res}/\sigma'_v$ (Figure 4). Approximately half of the values fall in the range 0.10-0.20 with isolated maximums near 0.30.

The same depth ranges as for the state parameters are used to perform frequency analyses, which are shown in Figure 5. It is observed that all the selected data entail $s_{u,res}/\sigma_v < 0.30$, with a mean value $s_{u,res}/\sigma_v \cong 0.11$. Results are compared with the best-practice trend values reported by Jefferies and Been (2016) considering the chosen design value $\psi \cong 0.02$: for stiff soils a $s_{u,res}/\sigma_v$ of 0.07 is expected, while intermediate soils entail a value of 0.13. It is shown that these values agree very well with those interpreted from sleeve friction measurements and covers a likelihood of occurrence between 15 and 65 %.

It must be mentioned that a recent correlation between $s_{u,res}/\sigma_v$ and $Q_{tn,cs}$ (after Robertson, 2017) was also evaluated. However, results are disregarded, as the achieved mean value is $s_{u,res}/\sigma_v \cong 0.03$. This can be explained by the fine content of the tailings and its subsequent undrained response during the cone penetration, which significantly reduces $Q_{tn,cs}$.

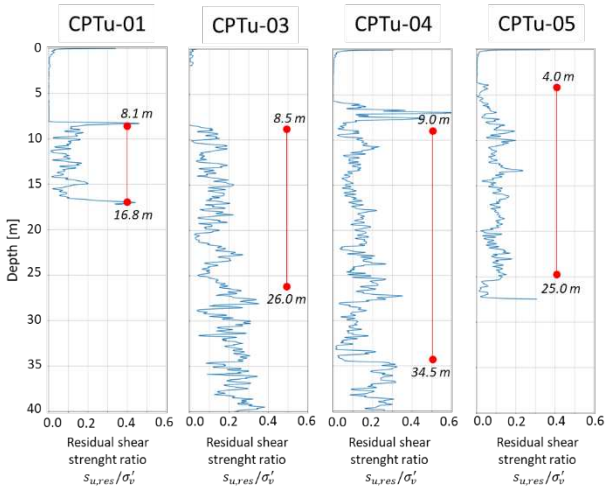

Figure 4. Residual shear strength ratio (assuming the cone sleeve friction) distribution at each CPTu sounding, .

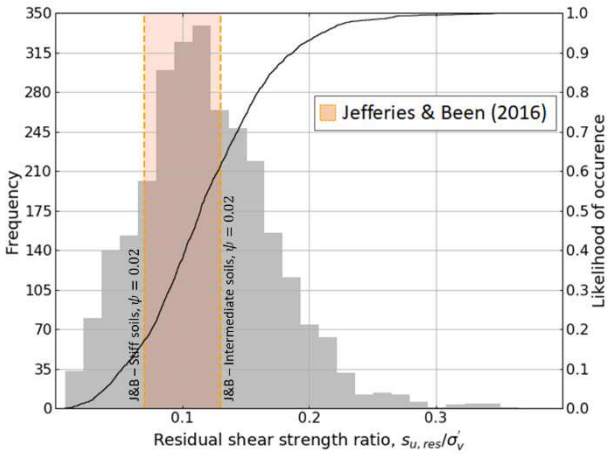

Figure 5. Residual shear strength ratio frequency and cumulative frequency analysis.

4 CONSTITUTIVE MODEL CALIBRATION

The Hardening Soil with Small-strain Stiffness (HSS) constitutive model (Schanz T. & Vermeer 1999; Benz 2006), implemented in Plaxis 2020, is used to simulate the staged construction and to analyze flow liquefaction triggers.

To properly capture undrained strain-softening using the HSS model, the strategy proposed by Sottile et. al. (2020) is followed. In a nutshell, the strategy is based on the fact that undrained shear occurs at constant volume, so that elastic expansion and plastic contraction must balance. In other words, undrained shear imposes $\dot{\epsilon}_v = \dot{\epsilon}_v^e + \dot{\epsilon}_v^p = 0$ so that adjusting the stiffness parameters that control elastic volumetric strain $\dot{\epsilon}_v^e$ and plastic volumetric strain $\dot{\epsilon}_v^p$ allows for capturing both peak and residual undrained shear strength ratios.

The calibration is performed in stages. Effective strength parameters (c', ϕ') are calibrated from CIUC tests. Small-strain stiffness parameters (G_0^{ref}, m) are calibrated from shear wave velocities measured from sCPTu tests and checked against data from Shuttle & Jefferies (2016) for silt-like tailings. Stiffness parameters ($E_{oed}^{ref}, E_{ur}^{ref}$) are calibrated from CRS oedometer tests Other parameters, such as $\gamma_{0.7}$, ν'_{ur}, K_0^{nc} and R_f are obtained from experience and recommendations from the literature.

HSS is not implemented in a critical state framework, therefore, the state parameter cannot be directly used as input defined because the void ratio is not a state variable. Thus, the second stage of calibration consists of adjusting the secant reference stiffness parameter E_{50}^{ref} that controls the shear-induced plastic volumetric strains to reproduce the peak/residual shear strength ratio for triaxial and direct simple shear stress paths.

For $\psi = 0.02$, Jefferies & Been (2016) suggest best-practice values for shear strength ratios of $0.20 < s_{u,peak}/\sigma'_v < 0.35$ and $0.07 < s_{u,res}/\sigma_v < 0.13$. With the set of parameters shown in Table 1, HSS predicts values that are within this range, as proven by the element test simulations explained below:

- K0-consolidated undrained triaxial compression (CK0UC) numerical tests are performed for three pre-shearing vertical effective stresses $\sigma'_{vo} = 100|250|500\ kPa$. Results are shown in Figure 6. The peak deviatoric stresses are 46, 114 and 228 kPa for the three stress levels respectively, entailing a normalized value $s_{u,peak}/\sigma'_v = 0.23$. The residual deviatoric stresses are 13, 33 and 66 kPa, respectively; entailing $s_{u,res}/\sigma'_v \sim 0.07$.
- Monotonic direct simple shear (MDSS) numerical tests are performed for the same vertical effective stresses; results are shown in Figure 7. The peak shear stresses are 23, 57 and 113 kPa for the three stress levels, entailing a normalized value $s_{u,peak}/\sigma'_v = 0.23$. The residual deviatoric stresses are 10, 26 and 54 kPa, respectively; entailing $s_{u,res}/\sigma'_v \sim 0.10$.

Table 1. HSS model parameters for tailings.

Parameters	Symbol	Value	Unit
Unit weight	γ	21.0	kN/m^3
Effective cohesion	c'	1.0	kPa
Friction angle	ϕ'	36.0	°
Initial shear modulus	G_0^{ref}	50.0	MPa
Reference shear strain	$\gamma_{0.7}$	1E-4	-
Unload ref stiffness	E_{ur}^{ref}	60.0	MPa
Secant ref stiffness	E_{50}^{ref}	3.5	MPa
Oedometric ref stiffness	E_{oed}^{ref}	9.0	MPa
Stress exponent	m	0.75	-
Poisson's ratio	ν'_{ur}	0.20	-

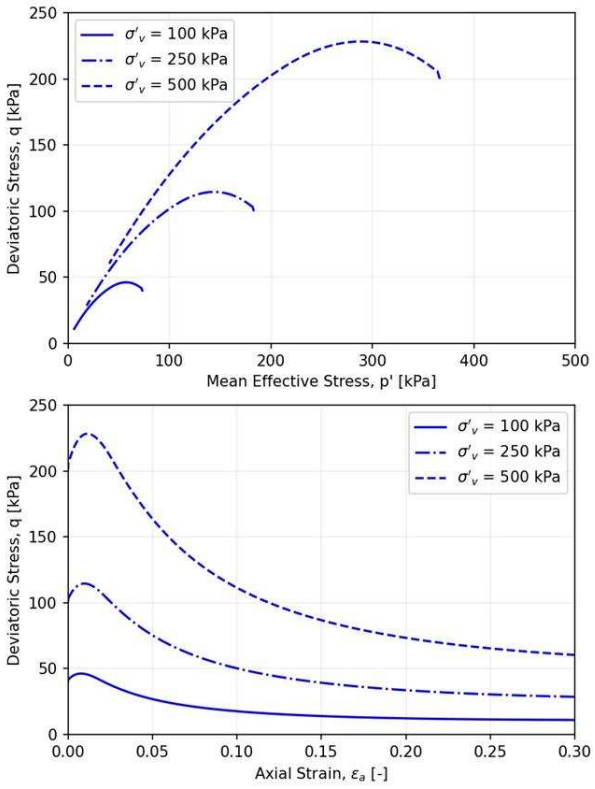

Figure 6. CK0UC elemental numerical tests simulations using HSS.

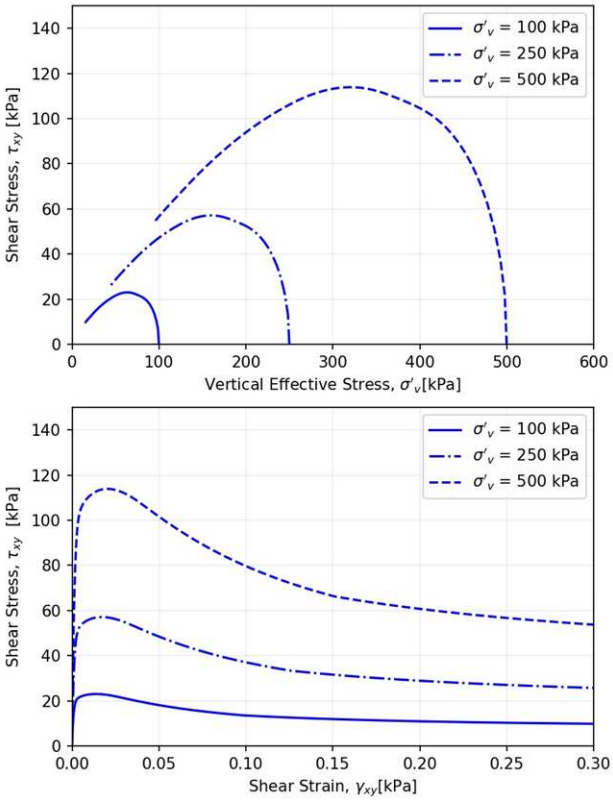

Figure 7. MDSS elemental numerical tests simulations using HSS.

5 NUMERICAL MODELLING

5.1 *Geometry and mesh*

The geometry and finite element mesh of the model is presented in Figure 8. The model has a total width of 650 m and a maximum height of 110 m. A total of 8954 triangular 15-node elements are used, with a maximum size of 21.6 m and a minimum size of 0.08 m. The phreatic surface configuration is obtained from a steady-state flow calculation at each stage.

5.3 *Modelling sequence*

The modelling is performed in the following sequence: i) initialization of stress at the foundation; ii) construction of the starter dam; iii) deposition of tailings up to the crest of the starter dam; iv) construction of rockfill and embankment raises; v) upstream raises and tailings deposition until the dam crest reaches the final elevation. At this point, flow liquefaction triggers A and B are analyzed. Trigger A applies a load at the current dam crest; this aims to represent heavy traffic loads or stockpiled material loads during regular mine operation. Trigger B applies a contraction -by means of a compressive horizonal strain- at the toe of the upstream embankment raises; this aims to represent eventual movements due to an accidental excavation during the buttress construction or a sudden loss/collapse of material due to piping. Then, the staged construction of the buttress is simulated using lifts of 0.7 m/day. Trigger C is analyzed similar to trigger A but with the buttress in place. A summary of the modelling sequence is presented in Figure 9. For simplicity, not all stages are shown.

It must be mentioned that all the trigger analyses are done considering an undrained behavior of the tailings material (i.e., nil volumetric strains with subsequent excess pore pressures generation during shearing) and conservatively assume that the material is saturated above the phreatic surface.

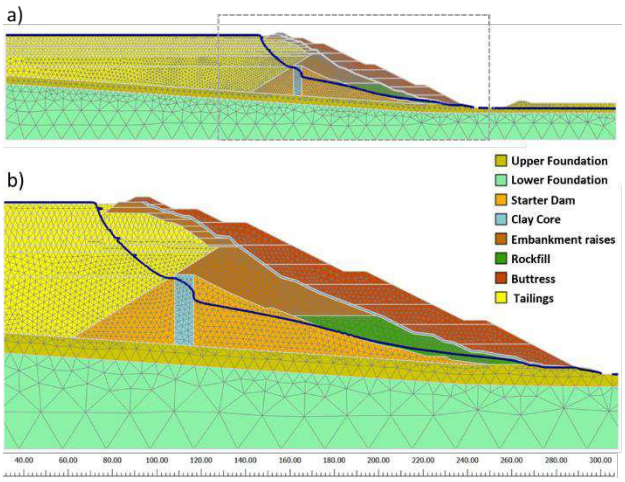

Figure 8. Model geometry and mesh. a) Complete model. b) Zoom in.

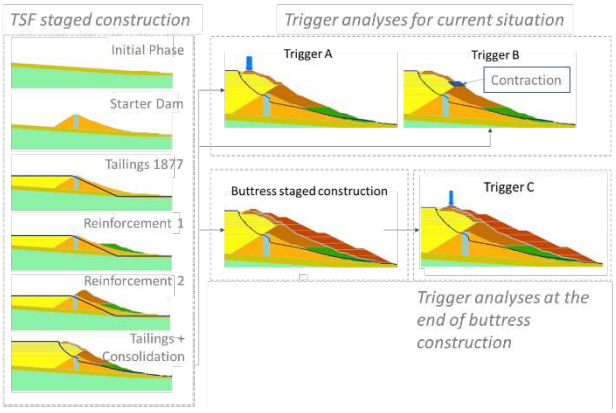

Figure 9. Numerical modelling sequence.

5.4 *Results*

The results of the analyses considering the three triggers described in Figure 9 are summarized as follows:

Trigger A: failure is achieved by applying an undrained load of 30 kPa at the current TSF dam crest. Contours of excess pore water pressures and incremental deviatoric strains are shown in Figure 10 a) and b) respectively, both associated with the load at failure. The failure surface starts near the embankment material and propagates through the tailings towards the dam crest. An increase of excess pore water pressures appears along the failure surface, suggesting that tailings might have strain-softened.

It must be mentioned that negligible displacements occur for loads of 10 and 20 kPa applied in previous stages. When the load is increased to 30 kPa, a sudden jump in the displacement is observed, which is associated to significant localized shear strains increments (Figure 10 b)). This sudden and significant increase in displacements caused by the small increase in the load (10 kPa) suggests that the failure can occur in a brittle manner. It should be noted that loads of about 30 kPa on the crest of the dam are plausible in regular mine operation. The interpretation of the simulation results supports the recommendations of not raising the current embankment before building the stabilization buttress as well as to avoid heavy traffic loads on the dam crest.

Trigger B: failure is achieved by applying a 0.5% horizontal contraction to the current TSF upstream toe; in terms of horizontal displacements, this is approximately 3 cm towards downstream. Contours of excess pore water pressures and incremental shear strains are shown in Figure 11 a) and b) respectively, both associated to the horizontal contraction at failure. These are similar to the results from Trigger A (Figure 10 a) and b)). An increase in the horizontal contraction from 0.4% to 0.5% will cause a rapid and significant increase in the

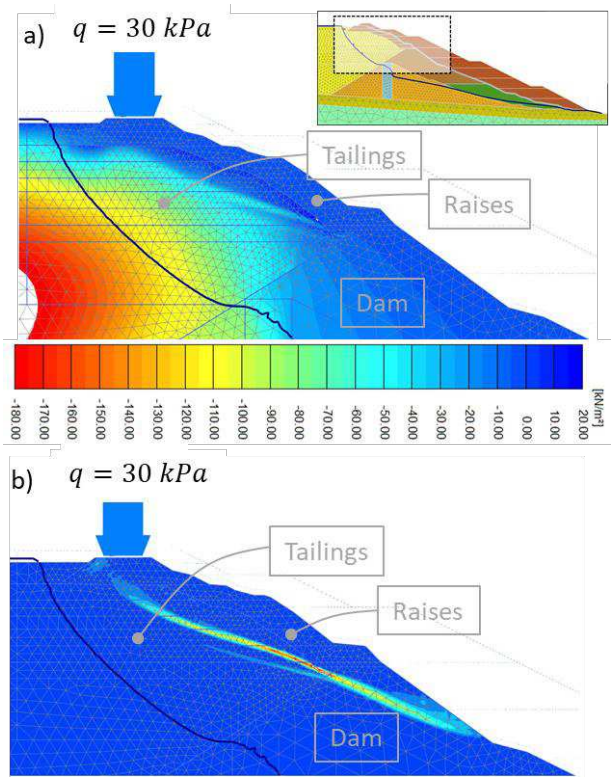

Figure 10. Trigger A analyses – load at current condition. a) excess pore pressure contour at failure; b) shear strain contours at failure.

horizontal displacements associated with the localized shear strains and excess of pore water pressures shown in Figure 11 a) and b). Therefore, a 0.5% horizontal contraction is considered to trigger the failure in the simulations. This analysis shows that special care must be taken in the upstream toe area during buttress construction, as failure can occur with very little or no observable warning. Stripping of the foundation for the buttress should be done with care to ensure that the toe of the existing dam is not excavated.

Five gauss points (A to E) are chosen to study the stress-strain-strength behavior along the failure for Trigger B (Figure 11). The deviatoric stresses and the mean effective stresses are normalized by the pre-triggering vertical effective stress. The correspondent stress paths, and stress-strain response are shown in Figure 12. It is observed that: i) points D and E have similar stress ratios before the triggering event and show pre-peak hardening while strained, while point A, B and C have a higher initial stress ratio and shows no pre-peak hardening; ii) the effective stress paths are qualitatively in agreement to the analogous CK0UC results shown in Figure 6, for which the mobilized stress is close to the undrained peak strength; iii) the undrained peak shear strength ratios for all points range between 0.27 and 0.35, which is slightly higher than the 0.23 achieved for the elemental numerical tests, and can be attributed to a higher initial stress ratio (i.e. before doing the triggering analyses); iv) the residual shear strength ratios for points B, C, D and E are in agreement with those reported for the elemental numerical tests ($s_{u,res}/\sigma'_v = 0.10$), which proves that the behavior captured by HSS can be normalized; however, point A shows higher peak and residual strength ratios, which can be attributed to its initial stress state and its closeness to the raises material.

Trigger C: the simulation results considering this event did not show failures related to loss-of-containment. The failure was only achieved by the bearing capacity of a load of 250 kPa applied under undrained conditions, immediately after the buttress was completed (Figure 13 a)). This very high, unrealistic load shows the robustness of the buttress design.

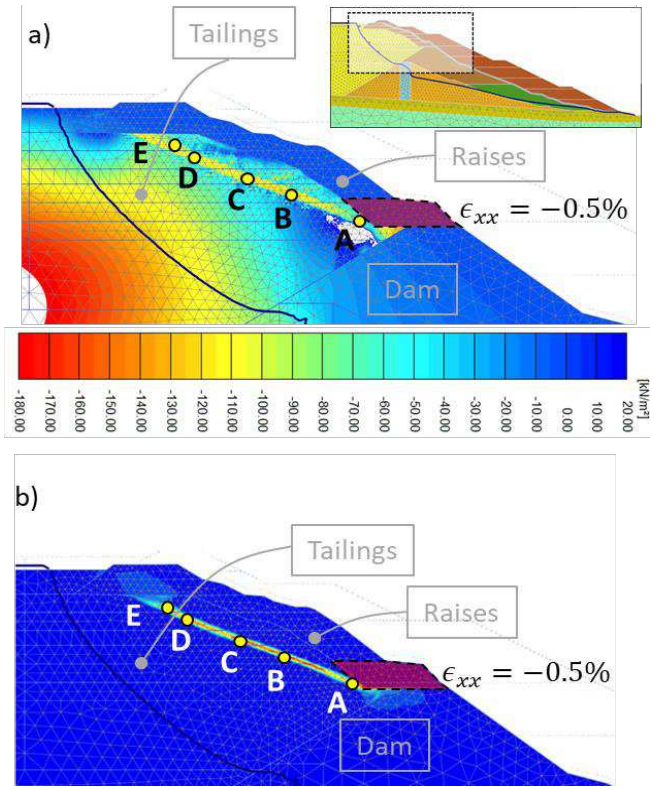

Figure 11. Trigger B analyses – toe deformation at current condition. a) excess pore pressure contour at failure; b) shear strain contours at failure.

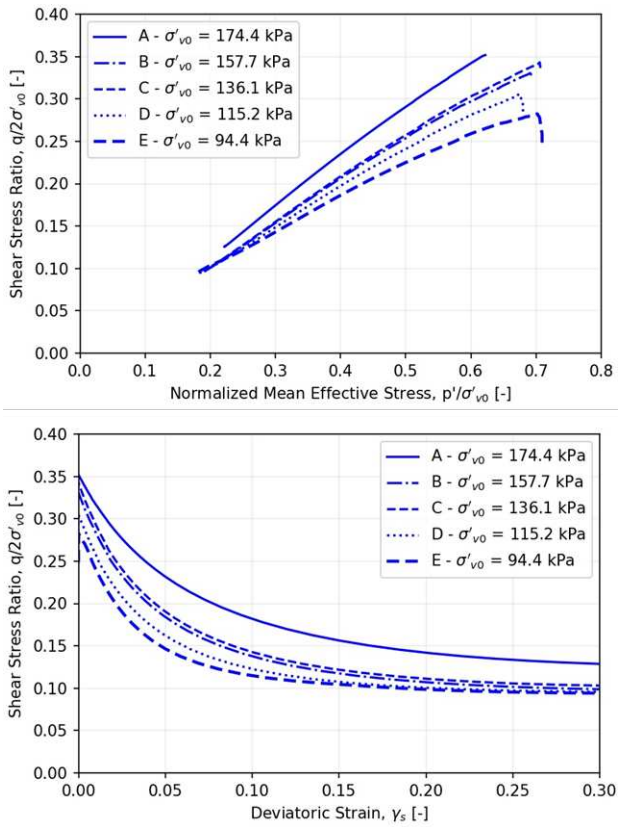

Figure 12. Trigger B analyses – toe deformation at current condition. Normalized stress paths and stress-strain at points A, B C, D and E;

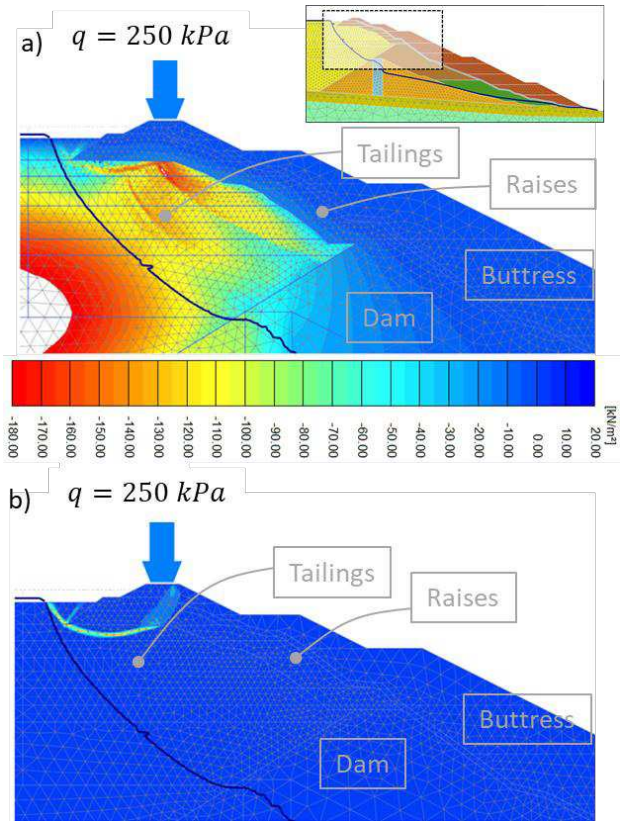

Figure 13. Trigger C analyses – load after building the buttress. a a) excess pore pressure contour at failure; b) shear strain contours at failure.

6 CONCLUSIONS

A finite element analysis is performed to assess the geotechnical stability of a TSF before, during and after construction of the stabilization buttress. Specifically, the analysis was performed to: i) evaluate the vulnerability of the dam to failure due to liquefaction of tailings in its current conditions; and ii) verify that the construction of a buttress helps to avoid failures related to loss-of-containment.

An analysis of CPTu data is done to estimate the state parameter distribution at the tailings below the dam crest using the screening methods proposed by Robertson (2010) and Jefferies & Been (2016) with Plewes (1992) correlation. All the soundings entail predominantly contractive states; a proposed design value (for probability of exceedance lower than 35%) is $\psi = 0.02$. Moreover, the residual shear strength ratio distributions are computed along all soundings, conservatively assuming the residual shear strength equal to the measured cone sleeve friction and normalizing by the vertical effective stress; the mean value is approximately 0.11.

State parameter interpretation suggest that tailings are contractive, and also the material is near saturated; thus, prone to strain-softening at large strains during undrained shearing. To properly capture this behavior using the HSS model, the calibration strategy proposed by Sottile et. al. (2020) is followed. , The strategy is based on the fact that undrained shear occurs at constant volume, so that elastic expansion and plastic contraction must balance, so that adjusting the stiffness parameters that control elastic volumetric strain $\dot{\epsilon}_v^e$ and plastic volumetric strain $\dot{\epsilon}_v^p$ allows for realistically capturing both peak and residual undrained shear strength ratios. An HSS parameter set is chosen such that simulated undrained strengths ratios are $s_{u,peak}/\sigma_v' \sim 0.23$ and $s_{u,res}/\sigma_v' \sim 0.07 - 0.10$, in agreement with recommendations from the literature and residual strengths interpreted from CPTu sleeve friction measurements.

The finite element analysis performed for the current condition of the dam suggest that static liquefaction of the tailings can be triggered by very small displacements. This indicates that a sudden onset of tailings liquefaction can occur with very little warning compromising the stability of the dam in its current condition; i.e., it is vulnerable to failure due to liquefaction of the tailings. Specifically, the analysis showed that liquefaction of the upper 20 m of the exiting dam could be triggered by:

A surface load as low as 30 kPa (equivalent to a ~1.5 m thick earth fill), if applied rapidly at the crest of the existing dam; or by small displacements (less than 3 cm) of the toe of the upstream-raised embankment of the current dam.

The practical consequences of these results are that: i) the crest of the current dam must not be raised until the stabilization buttress is constructed; ii) heavy equipment transit on the crest of the current dam must not be allowed until the stabilization buttress is complete; and iii) no materials are to be stockpiled at the crest of the dam during construction.

7 REFERENCES

ANCOLD (2019) Australian National committee on Large Dams. Guidelines on Tailings Dams. Planning, Design, Construction, Operation and Closure. Addendum. July, 2019. Benz, T (2006). "Small-strain Stiffness of Soils and its Numerical Consequences", PhD Thesis, Stuttgart University.

Jefferies, M & Been, K. (2016). "Soil liquefaction: a critical state approach, 2nd edition".

Plewes, H.D., Davies, M.P., and Jefferies, M.G., (1992.). CPT based screening proce- dure for evaluating liquefaction susceptibility. In Proceedings of the 45 th Canadian Geotechnical Conference, pp. 41-49.

Robertson, P.K. (2009). "Interpretation of cone penetration tests — a unified approach". Canadian Geotechnical Journal, 2009, 46(11): 1337-1355.

Robertson, P.K. (2010). "Evaluation of flow liquefaction and liquefied strength using the cone penetration test". Journal of Geotechnical and Geoenvironmental Engineering, ASCE.

Robertson (2017). "Evaluation of Flow Liquefaction: influence of high stresses". Proceedings from 3rd International Conference on Performance Based Design in Earthquake Geotechnical Engineering, Vancouver.

Santamarina C., Torres-Cruz L.A. and Bachus R.C. (2019). Why coal ash and tailings dam disas-ters occur. Science, 364(6440): 526-528. DOI: 10.1126/science.aax1927.

Schanz T. & Vermeer P.A (1999). The Hardening soil model: Formulation and verification, Beyond 2000 in Computational Geotechnics, Rotterdam, Netherlands, 281-290.

Sottile M., Cueto, I. & Sfriso, A. (2020). A simplified procedure to numerically evaluate triggering of static liquefaction in upstream-raised tailings storage facilities. COBRAMSEG, Campinhas.